Thin Solid Films 518 (2010) 6339–6342

Contents lists available at ScienceDirect

Thin Solid Films

journal homepage: www.elsevier.com/locate/tsf

Light-emitting characteristics of organic light-emitting diodes with the MoO_x-doped NPB and C_{60}/LiF layer

Jae Wook Kwon, Jong Tae Lim, Geun Young Yeom *

School of Advanced Materials Science and Engineering, Sungkyunkwan University, Suwon 440-746, South Korea

ARTICLE INFO

Available online 18 January 2010

Keywords:
Ohmic contact
Molybdenum oxide
Organic light-emitting diode
Electronic structure
Ultraviolet photoemission spectroscopy

ABSTRACT

The hole ohmic properties of the MoO_x-doped NPB layer have been investigated by analyzing the current density–voltage properties of hole-only devices and by assigning the energy levels of ultraviolet photoemission spectra. The result showed that the performance of organic light-emitting diodes (OLEDs) is markedly improved by optimizing both the thickness and the doping concentration of a hole-injecting layer (HIL) of N, N′-diphenyl-N, N′-bis(1-naphthyl)-1,1′-biphenyl-4,4′-diamine (NPB) doped with molybdenum oxide (MoO_x) which was inserted between indium tin oxide (ITO) and NPB. For the doping concentration of above 25%, the device composed of a glass/ITO/MoO_x-doped NPB (100 nm)/Al structure showed the excellent hole ohmic property. The investigation of the valence band structure revealed that the p-type doping effects in the HTL layer and the hole concentration increased at the anode interfaces cause the hole-injecting barrier lowering. With both MoO_x-doped NPB as a hole ohmic contact and C_{60}/LiF as an electron ohmic contact, the device, which is composed of glass/ITO/MoO_x-doped NPB (25%, 5 nm)/NPB (63 nm)/Alq_3 (37 nm)/C_{60} (5 nm)/LiF (1 nm)/Al (100 nm), showed the luminance of about 58,300 cd/m^2 at the low bias voltage of 7.2 V.

1. Introduction

Organic light-emitting diodes (OLEDs) have been developed due to their possible application for cheap, lightweight, flexible, large area lightings and displays [1]. One of the crucial issues in the physics and operation of the OLEDs is the carrier injection from the electrodes into the emitting layer. The injection probability is strongly dependent on the mismatch between the Fermi levels (E_F) of the electrodes and the relevant levels for conduction in the OLED, i.e., the injection barrier heights [2]. The fact that these are typically not pinned in organic (or inorganic)/metal contacts [3–7], and are thus strongly dependent on the work function of the electrode, allows the minimization of such barriers by employing low work-function metals as cathodes [8] and high work-function conductors as anodes [9]. This asymmetry in the work functions also results in a large asymmetry of the barrier heights to hole and electron injection. Therefore, developing the efficient carrier-injecting layer is necessary to obtain a long life-time and high luminous efficiency as well as a low power conception [9].

Among these carrier-injecting layers, molybdenum oxide (MoO_x) is a material frequently used as the hole-injecting layer (HIL) between a tin-doped indium oxide (ITO) layer and a hole-transporting layer (HTL) [4–7,10]. Also, MoO_x is used as a p-type dopant in a HTL to reduce the driving voltage [5,7,10]. T. Matsushima et al. recently demonstrated that the use of MoO_x as a HIL, inserted between ITO and N, N′-diphenyl-N, N′-bis(1-naphthyl)-1,1′-biphenyl-4,4′-diamine (NPB), leads to the formation of an ohmic contact at the ITO/MoO_x/NPB interfaces due to electron transfers from ITO to MoO_x and from NPB to MoO_x [6]. Also, they proved that the formation of an ohmic contact not only provides the low driving voltage but leads to a stable life-time of the OLEDs [7]. Meanwhile, X.D. Feng et al. reported that fullerene (C_{60}) acts as a highly conductive electron-transporting layer (ETL), forming an electron ohmic contact with a lithium fluoride (LiF)/Al bi-layer cathode [11]. Forming these ohmic interfaces between electrodes and organics could be beneficial for obtaining the high-performance OLED and for enhancing the light-emitting efficiency.

In this study, the light-emitting characteristics of all ohmic OLED have been investigated by inserting both the MoO_x-doped NPB layer as the hole ohmic contact and the C_{60}/LiF layer as the electron ohmic contact. By varying the MoO_x doping concentration in the MoO_x-doped NPB layer, the mechanism for forming the hole ohmic contact was investigated by analyzing the current density–voltage characteristics of the hole-only devices composing of glass/ITO/MoO_x-doped NPB/Al and by assigning the energy levels in the MoO_x-doped NPB/anode interfaces. Also, the correlation between the driving performance in all ohmic devices and the interfacial property of the MoO_x-doped NPB thin film is discussed.

2. Experimental

The structure of all ohmic OLEDs was glass/ITO (about 10 Ω/square, Geomatec Co. Ltd.)/MoO_x-doped NPB (25%, *x* nm)/NPB (68–*x* nm)/Alq_3 (37 nm)/C_{60} (5 nm)/LiF (1 nm)/Al (100 nm). The thicknesses of

* Corresponding author. Fax: +82 31 299 6565.
E-mail address: gyyeom@skku.edu (G.Y. Yeom).

0040-6090/$ – see front matter © 2010 Elsevier B.V. All rights reserved.
doi:10.1016/j.tsf.2009.12.108

MoO_x-doped NPB in Devices 0, 1, 2 and 3 were 0, 5, 10, and 15 nm, respectively. MoO_x-doped NPB/NPB/Alq_3/C_{60}/LiF/Al, consisting of NPB doped with MoO_x as a HIL, NPB as a HTL, tris(8-quinolinolato) aluminum (III) (Alq_3) as an emissive layer (EML), C_{60} as an electron-transporting layer, LiF as an electron-injecting layer, and aluminum (Al) as a cathode layer, was sequentially vacuum-deposited by using a thermal evaporator system. Then, the device fabricated was encapsulated by depositing a bead of epoxy around the edge of the substrate, sticking another piece of glass on the bead, and curing the epoxy in a dry nitrogen box. The emissive active area of the devices was $2.0 \times 2.0\ mm^2$.

The hole-only device was separately fabricated as the structure of glass/ITO/MoO_x-doped NPB (y%, 100 nm)/Al (100 nm). Here, the doping concentration (y%) of MoO_x was varied as 0, 5, 25, 50, 75, and 100%.

The current density–voltage–luminance characteristics were measured using a source-measure unit (2400, Keithley Instrument Inc.) while the emission intensities from the OLEDs devices were measured by using the photocurrent induced on a silicon photodiode (Oriel 71608) with a picoammeter (485, Keithley Instrument Inc.). The electroluminescence (EL) spectra of the as-fabricated devices were measured by using optical emission spectroscopy (PCM-420, SC Tech. Inc.). The ultraviolet photoemission spectroscopy (UPS) analyses were carried out at the 4B1 beam line of the Pohang Accelerator Laboratory in Korea. A ultraviolet source of the He I (21.2 eV) line was used. For the analysis, the MoO_x-doped NPB (10 nm) was deposited on p-Si substrates in a ultra-high vacuum system which was connected to the beam line in vacuum. The photoemission onset reflecting the vacuum level (VL) at the surface of all samples was measured by biasing the samples at −20 V. The incident photon energy was calibrated by measuring the Au 4f level of a clean Au surface.

3. Results and discussion

Fig. 1 shows the current density–voltage curves of the hole-only devices which have a ITO/MoO_x-doped NPB/Al devices structure, as a function of the MoO_x doping concentration. Here, the thickness of MoO_x-doped NPB was 100 nm. It is found that the ITO/MoO_x-doped NPB/Al device exhibits a perfectly linear line with the characteristics of a true ohmic contact at both the top and bottom interfaces, when the doping concentration is 25% and above. However, when the doping concentration of MoO_x is either below 5% or 100%, the current density–voltage curves show non-linear relationships. This fact reveals that these interfaces are typically not pinned at organic/metal contacts, and are thus strongly dependent on the doping concentration of MoO_x. To explain this correlation between the doping concentration and the cationic charge carrier density, W.-J. Shin et al. has investigated the formation of charge transfer complexes (CTCs) using ultraviolet spectroscopy [7]. His study showed that the broad absorption band around 1400 nm in the UV spectrum was clearly observed only for MoO_x-doped NPB films. Doping MoO_x (as electron acceptor) into NPB (as electron donor) forms easily charge transfer complexes between the host and dopant materials, leading to a marked increase in the free carrier concentration in the doped layers of 25% and above, when compared to the doped layers of 5% [12]. Similarly, the ohmic properties of the doped layer with the concentration of 25% and above shown in Fig. 1 is believed to be related to the formation of CTCs at the interface.

The investigation of the energy levels at the MoO_x-doped NPB films is important to understand the mechanism for a hole-injecting property near the HIL/anode interface, when changing the doping concentration of MoO_x. Fig. 2 shows UPS spectra of the pristine NPB and NPB doped with various MoO_x doping concentration deposited on the p-Si substrates. Fig. 2(a) shows the onset of the valence band spectra, representing the vacuum level of the surface. When compared to the vacuum level (VL) of pristine NPB, the VL is lowered about 1.0 eV for 25% and 75% of MoO_x in NPB. Fig. 2(b) and (c) show the valence spectra and the region around the highest occupied molecular orbital (HOMO) of MoO_x-doped NPB, respectively. Also, Fig. 3 exhibits the energy levels of the MoO_x-doped NPB layer of 10 nm-thick, obtained from the results of Fig. 2. As shown in the figures, the hole-injecting barrier, the energy difference between the Fermi level of the anode and the edge of HOMO of NPB, is about 1.1 eV. The ionization energy is measured as 5.4 eV, which is consistent with the previous report [13]. Figs. 2 and 3 also clearly show that NPBs doped with MoO_x maintain the main features of the valence spectra of

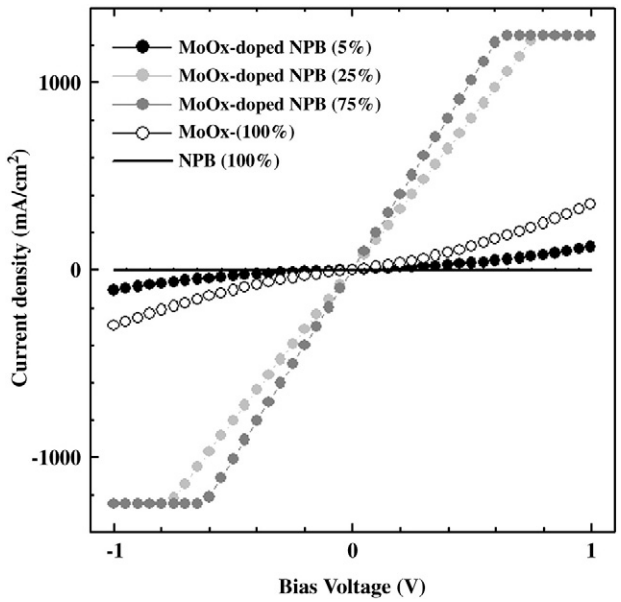

Fig. 1. Current density–voltage characteristics of the ITO/MoO_x-doped NPB/Al devices as a function of the MoO_x doping concentration in the 100 nm-thick NPB layer. The bias was applied to the bottom electrode in reference to the top grounding electrode.

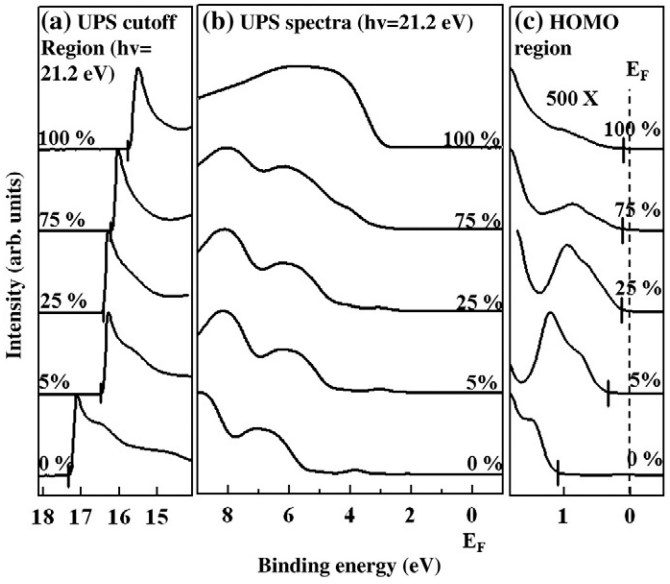

Fig. 2. Ultraviolet photoemission spectra of the MoO_x-doped NPB layer with various MoO_x doping concentration. (a) shows the onset of the valence band, representing the work function of the surface. (b) and (c) show the valence spectra and the region around HOMO of the MoO_x-doped NPB layers, respectively. A region around HOMO in (c) was magnified to the scale of 500 times. The values in the figures indicate the doping concentration of MoO_x in NPB.

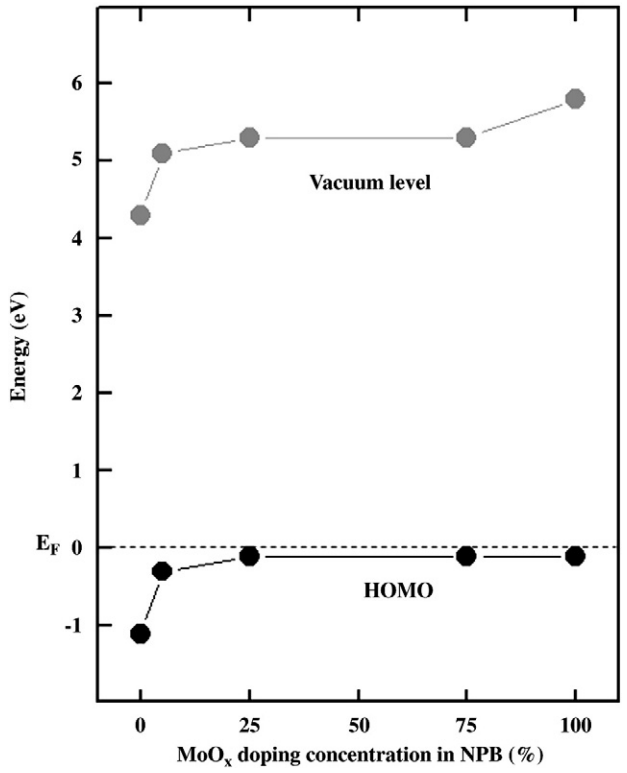

Fig. 3. Energy levels of the MoO_x-doped NPB layer (10 nm) as a function of doping concentration.

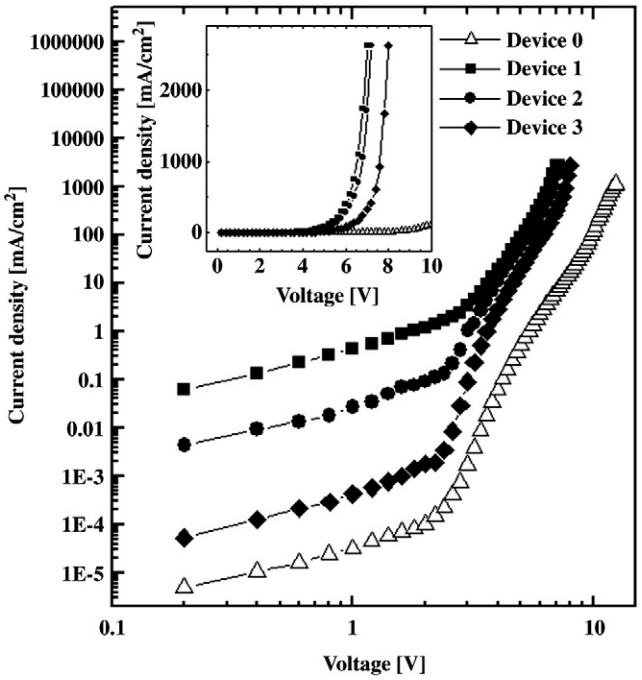

Fig. 4. Log*J* vs. Log*V* plot of Devices 0, 1, 2, and 3. The inset shows the current densities as a function of the forward bias voltage in Devices 0, 1, 2, and 3. The devices were composed of glass/ITO/MoO_x-doped NPB (25%, *x* nm)/NPB (68–*x* nm)/Alq_3 (37 nm)/C_{60} (5 nm)/LiF (1 nm)/Al (100 nm). MoO_x-doped NPB thicknesses of Devices 0, 1, 2, 3 were 0, 5, 10, and 15 nm, respectively.

pristine NPB but the position of HOMO as reference to that of pristine NPB shifts toward the Fermi level by 1.0 eV. The decrease in the energy difference between the Fermi level and the HOMO implied that the hole concentration increases in the NPB doped with MoO_x. Therefore, MoO_x can serve as a *p*-type dopant when it is mixed with NPB. Combined with shifts in the vacuum level and the HOMO, NPB doped with MoO_x not only reduces hole injection barriers by 1 eV but also increases the carrier concentration in the organic films, evidently explains the improvement in the device performance.

On the other hand, C.-I Wu et al. has claimed that the lowering of the HOHO level forward the Fermi level is because NPB molecules react with MoO_x [4]. And the reduction in the oxidation states of MoO_x results in the positive charge transfer to NPB. This process at the anode/organic interfaces helps the hole injections and virtually reduces the hole-injecting barrier height. At the high MoO_x dopant concentration of 25% and above, the top of the HOMO level aligns easily with the Fermi level, which implies more transition of insulating MoO_3 to metallic MoO_2. As shown in Fig. 3, the hole-injecting barrier at the doping concentration of 25% and above was only 0.1 eV.

To fabricate all ohmic devices, we used the layers of MoO_x-doped NPB (25%) as a hole ohmic contact as proven in Figs. 1 and 2 and C_{60} (5 nm)/LiF(1 nm) [11] as an electron ohmic contact. The device structure was composed of glass/ITO/MoO_x-doped NPB (25%, *x* nm)/NPB (68–*x* nm)/Alq_3 (37 nm)/C_{60} (5 nm)/LiF (1 nm)/Al (100 nm). The thicknesses of MoO_x-doped NPB in Devices 0, 1, 2 and 3 were 0, 5, 10, and 15 nm, respectively. The log*J*–log*V* plots of the all ohmic devices fabricated are shown in Fig. 4. As shown in the figure, at the low voltage of approximately below 2 V, the devices shifted to higher current density states and gradually showed the relationship from $J = V^{1.4}$ to $J = V^{1.2}$ as the thickness of MoO_x-doped NPB was decreased from 15 to 5 nm for the MoO_x doping concentration of 25%. This means that an hole-injecting property is improved and the hole concentration is increased at the ITO/NPB interface with the reduction of the thickness of MoO_x-doped NPB.

The inset of Fig. 4 shows the current density–voltage curves of Devices 0, 1, 2, and 3. It is clear that the devices with the MoO_x doped NPB between the ITO and NPB demonstrate better current efficiency. The use of MoO_x doped NPB certainly facilitates the injection of hole from ITO to NPB. The turn-on voltages (V_T) at the luminance of about 0.1 cd/m^2 for Devices 0, 1, 2 and 3 were 3.4, 2.6, 2.6, and 2.8 V, respectively. The current density–voltage–luminance characteristics for Devices 0, 1, 2, and 3 are also summarized in Table 1. As shown in Table 1, Device 1 shows the high luminance of 1000 cd/m^2 (L_{1000}) and the high current density of 34.5 mA/cm^2 at the low voltage of 4.4 V. Also, Device 1 shows the high maximum luminance (L_{max}) of 58,300 cd/m^2 at the low voltage of 7.2 V.

Fig. 5 shows the power efficiency (η_{PE}) for Devices 0, 1, 2, and 3 measured as a function of the luminance. The results are also summarized in Table 1. As shown in Fig. 5 and Table 1, η_{PE} at L_{1000} was 1.1, 3.7, 3.4 and 2.6 lm/W, for Devices 0, 1, 2 and 3, respectively. When the device characteristics such as V_T, J_{1000}, L_{max}, and η_{PE} were compared

Table 1
Current density–voltage–luminance characteristics of the devices, which have the structure of glass/ITO/MoO_x-doped NPB (*x* nm)/NPB (68–*x* nm)/Alq_3 (37 nm)/C_{60} (5 nm)/LiF (1 nm)/Al (100 nm). The thicknesses of the MoO_x-doped NPB layer in Devices 0, 1, 2, 3 are 0, 5, 10, 15 nm, respectively.

Devices	Thickness of the MoO_x-doped NPB layer (25, *x* nm)	V_T at 0.1 cd/m^2	η_{PE} (lm/W) at 1000 cd/m^2	L_{max} (cd/m^2)	*V* (V) at 1000 cd/m^2
0	0	3.0	1.1	235 at 7.2 V	8.2 at 19.8 mA/cm^2
1	5	2.6	3.7	58,300 at 7.2 V	4.4 at 34.5 mA/cm^2
2	10	2.6	3.4	47,500 at 7.2 V	4.6 at 33.2 mA/cm^2
3	15	2.8	2.6	14,700 at 7.2 V	5 at 27.4 mA/cm^2

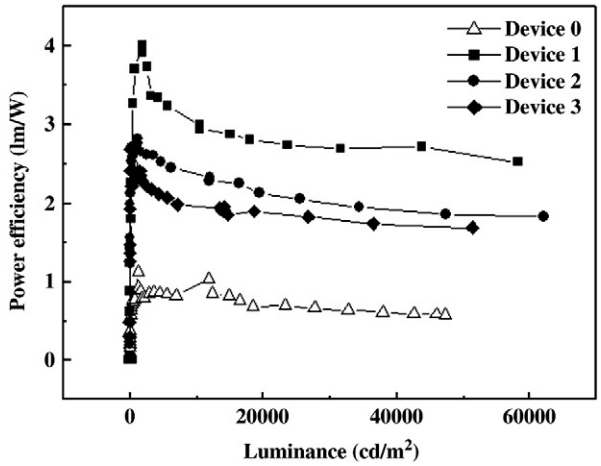

Fig. 5. Power efficiency as a function of luminance. The devices were composed of glass/ITO/MoO_x-doped NPB (25%, *x* nm)/NPB (68–*x* nm)/Alq_3 (37 nm)/C_{60} (5 nm)/LiF (1 nm)/Al (100 nm). MoO_x-doped NPB thicknesses of Devices 0, 1, 2, 3 were 0, 5, 10, and 15 nm, respectively.

among the devices used in this paper, Device 1 with the MoO_x-doped NPB (25%, 5 nm) showed the best light-emitting characteristics.

4. Conclusions

The all ohmic device with a structure of glass/ITO/MoO_x-doped NPB (25%, 5 nm)/NPB (63 nm)/Alq_3 (37 nm)/C_{60} (5 nm)/LiF (1 nm)/Al (100 nm) showed the high light-emitting characteristic with L_{max} of 58,300 cd/m^2 at the low forward bias voltage of 7.2 eV. UPS spectra explain that there are chemical reaction and electronic interaction between MoO_x and NPB, resulting in p-type doping in NPB. Also, the hole-only devices proved that there is the hole–ohmic property at the doping concentration of 25% and above. In addition, we found that the interface effects play a major role in lowering the operating voltage and enhancing the stability of the OLEDs with a MoO_x-doped NPB.

Acknowledgments

This research was supported by a grant (PAD-4) from Information Display R&D Center, one of the 21st Century Frontier R&D Program funded by the Ministry of Knowledge Economy of Korean government. Also, this work was supported by Pohang Accelerator Laboratory in Korea.

References

[1] S.R. Forrest, Nature 428 (2004) 911.
[2] H. Ishii, K. Sugiyama, E. Ito, K. Seki, Adv. Mater. 11 (1999) 605.
[3] J. Campbell, J. Vac. Sci. Technol. A 21 (2003) 521.
[4] C.-I. Wu, C.-T. Lin, G.-R. Lee, T.-Y. Cho, C.-C. Wu, T.-W. Pi, J. Appl. Phys. 105 (2009) 33717.
[5] T. Matsushima, C. Adachi, J. Appl. Phys. 103 (2008) 34501.
[6] T. Matsushima, Y. Kinoshita, H. Murata, Appl. Phys. Lett. 91 (2007) 253504.
[7] W.-J. Shin, J.-Y. Lee, J.C. Kim, T.-H. Yoon, T.-S. Kim, O.-K. Song, Org. Electron. 9 (2008) 333.
[8] M.G. Mason, C.W. Tang, L.-S. Hung, P. Raychaudhuri, J. Madathil, D.J. Giesen, L. Yan, Q.T. Le, Y. Gao, S.-T. Lee, L.S. Liao, L.F. Cheng, W.R. Salaneck, D.A. dos Santos, J.L. Brédas, J. Appl. Phys. 89 (2001) 2756.
[9] X. Zhou, M. Pfeiffer, J.S. Huang, J. Biochwitz-Nimoth, D.S. Qin, A. Werner, J. Drechsel, B. Maennig, K. Leo, Appl. Phys. Lett. 81 (2002) 922.
[10] G. Xie, Y. Meng, F. Wu, C. Tao, D. Zhang, M. Liu, Q. Xue, W. Chen, Y. Zhao, Appl. Phys. Lett. 92 (2008) 93305.
[11] X.D. Feng, C.J. Huang, V. Lui, R.S. Khangura, Z.H. Lu, Appl. Phys. Lett. 86 (2005) 143511.
[12] M. Pfeiffer, A. Beyer, K. Leo, Appl. Phys. Lett. 73 (1998) 3202.
[13] J.X. Tang, C.s. Lee, S.T. Lee, J. Appl. Lett. 101 (2007) 64504.